Open Access Articles

Long-term explosive degassing and debris flow activity at West Mata submarine volcano

Oregon State
UNIVERSITY

Correspondence to:
R. P. Dziak,
Robert.P.Dziak@noaa.gov

Long-term explosive degassing and debris flow activity at West Mata submarine volcano

R. P. Dziak[1], D. R. Bohnenstiehl[2], E. T Baker[3], H. Matsumoto[1], J. Caplan-Auerbach[4], R. W. Embley[5], S. G. Merle[1], S. L. Walker[3], T.-K. Lau[1], and W. W. Chadwick Jr.[1]

[1]Cooperative Institute for Marine Resource Studies/Oregon State University, NOAA/Pacific Marine Environmental Laboratory, Hatfield Marine Science Center, Newport, Oregon, USA, [2]Department of Marine, Earth and Atmospheric Sciences, North Carolina State University at Raleigh, Raleigh, North Carolina, USA, [3]Joint Institute for the Study of Atmosphere and Oceans, NOAA/Pacific Marine Environmental Laboratory, Seattle, Washington, USA, [4]Department of Geology, Western Washington University, Bellingham, Washington, USA, [5]NOAA/Pacific Marine Environmental Laboratory, Hatfield Marine Science Center, Newport, Oregon, USA

Abstract West Mata is a 1200 m deep submarine volcano where explosive boninite eruptions were observed in 2009. The acoustic signatures from the volcano's summit eruptive vents *Hades* and *Prometheus* were recorded with an in situ (~25 m range) hydrophone during ROV dives in May 2009 and with local (~5 km range) moored hydrophones between December 2009 and August 2011. The sensors recorded low frequency (1–40 Hz), short duration explosions consistent with magma bubble bursts from *Hades*, and broadband, 1–5 min duration signals associated with episodes of fragmentation degassing from *Prometheus*. Long-term eruptive degassing signals, recorded through May 2010, preceded a several month period of declining activity. Degassing episodes were not recorded acoustically after early 2011, although quieter effusive eruption activity may have continued. Synchronous optical measurements of turbidity made between December 2009 and April 2010 indicate that turbidity maxima resulted from occasional south flank slope failures triggered by the collapse of accumulated debris during eruption intervals.

1. Introduction

Even though ~75% of Earth's volcanism occurs below the sea surface, many questions remain on the longevity and acoustic characteristics of explosive seafloor eruptions. To date, only two active eruptions have been visually observed at deep ocean (>500 m) volcanoes, and then only over periods of hours to days [*Chadwick et al.*, 2008; *Resing et al.*, 2011]. Moreover, prolonged monitoring of the regional seismicity in the vicinity of submarine volcanoes to infer the tectonic context of the magma system is rarely undertaken because of the difficulty of maintaining long-term deployments of sensors in the deep ocean. The discovery of the actively erupting West Mata Volcano [*Resing et al.*, 2011] in the NE Lau Basin near Samoa offered a rare opportunity to investigate a deep ocean, explosive degassing eruption. Video images collected by a remotely operated vehicle (ROV) provided unprecedented details on the dynamics of gas-driven eruptions at 1200 m depth [*Resing et al.*, 2011].

Here we present a 20 month long record of explosive eruptions at West Mata Volcano from two deployments of moored hydrophones (from the NOAA/Pacific Marine Environmental Laboratory). The first deployment, December 2009 to April 2010, utilized four instruments 5 to 20 km from the volcano's summit; these data were complemented by a water column turbidity sensor on the closest mooring (Figure 1). The second deployment, April 2010 to August 2011, reoccupied only the southern mooring location with a single hydrophone. These remote observations are supplemented by short-term (hours) in situ recordings from a bottom-deployed hydrophone (a GreenRidge Sciences Bprobe™) positioned on the summit during ROV dives in 2009. These acoustic time series provide a detailed account of submarine eruption signals, which are composed of short-duration eruptive bursts, longer-duration broadband explosions, and narrowband tremor with overtones. The character of these signals provides insights into explosive magma degassing at the volcano's summit vents. The hydrophones also recorded (over a 6 month period) the decline and apparent cessation of the long-term submarine eruption. The combined ash and hydrophone data describe repeated explosions followed by debris flows down the volcano's flank, which are important processes in the construction of the volcanic edifice and the regional dispersal of volcanic ash [*Clague et al.*, 2011; *Embley et al.*, 2014].
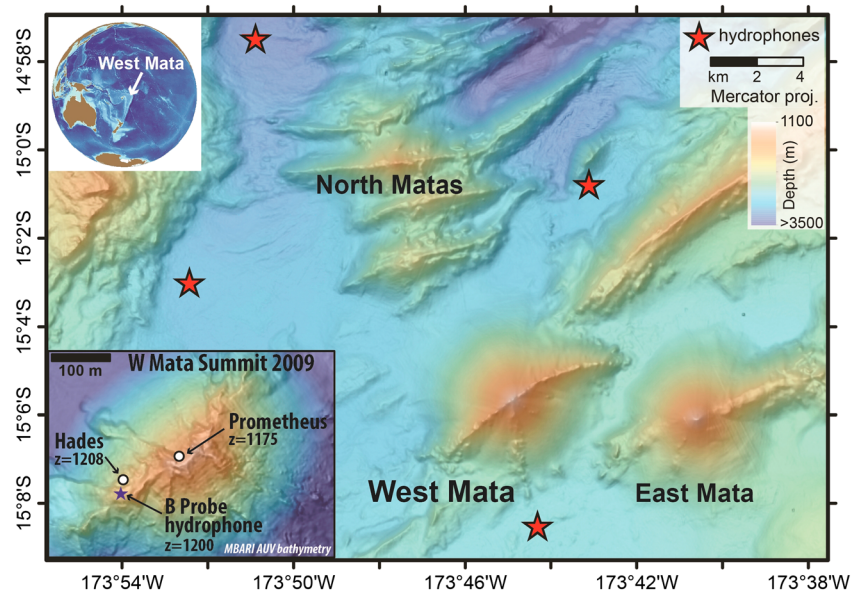
Figure 1. Maps showing bathymetry of West Mata Volcano and regional volcano-tectonic structures. North, West, and East Mata Volcanoes are part of en echelon volcano complex formed on a series of tear faults located south of American Samoa in the western Pacific Ocean. Red stars show locations of hydrophones moored 1–1.5 km off the seafloor. Inset is a small-scale view of West Mata showing the locations of actively erupting summit vents (*Hades* and *Prometheus*) and in situ hydrophone [after *Clague et al.*, 2011].

2. West Mata Tectonic Setting

The NE Lau Basin, adjacent to the northernmost part of the Tofua Arc formed by the subduction of the Pacific Plate beneath the Australian Plate, undergoes Earth's highest subduction rates and hosts the fastest-opening back-arc basin [*Bevis et al.*, 1995; *Zellmer and Taylor*, 2001]. The NE Lau Basin contains abundant recent submarine volcanism, with magma production likely driven by water released from the subducting slab [*Keller et al.*, 2008]. The 1200 m deep West Mata submarine volcano is located in the NE Lau Basin, midway between the Tonga Trench and the NE Lau Spreading Center (Figure 1). West Mata is one of nine elongate, en echelon volcanoes that have formed on tear faults in the oceanic crust [*Millen and Hamburger*, 1998]. Eruption activity at West Mata was discovered in 2008 during hydrothermal plume surveys of the NE Lau Basin that found anomalously high concentrations of dissolved H_2 and basaltic glass shards ~175 m above the summit [e.g., *Resing et al.*, 2011]. ROV dives at the volcano in 2009 confirmed it was in eruption, with explosive degassing at two summit vents named *Hades* and *Prometheus* (Figure 1, inset). West Mata erupts boninitic lava, a rarely observed, arc-fluid-enriched magma with relatively high water content and differentiated magmatic glasses that are relatively hot on eruption for its silica content as compared to most submarine magmas [*Rubin et al.*, 2013]. West Mata magma is also crystal rich (>40% by volume), making it relatively viscous.

3. Volcanic Explosion Signal Characteristics

The summit eruptive vents *Hades* and *Prometheus* observed during ROV dives in May 2009 exhibited very different styles of degassing eruptions. *Hades* produces frequent (~10–20 per minute) magma bubble bursts while *Prometheus* exhibited extensive fragmentation and a rapid degassing eruption style [*Resing et al.*, 2011; *Rubin et al.*, 2012].

Both the in situ and moored hydrophone records are dominated by broadband (1–110 Hz), explosion-like signals of 1–5 min durations with a rapid onset and termination (Figures 2a and 2b). These signals are consistent with the fragmentation degassing eruption style observed at *Prometheus* vent, where the fragmentation occurs episodically in the magma conduit during degassing pressure release events [*Chadwick et al.*, 2008].
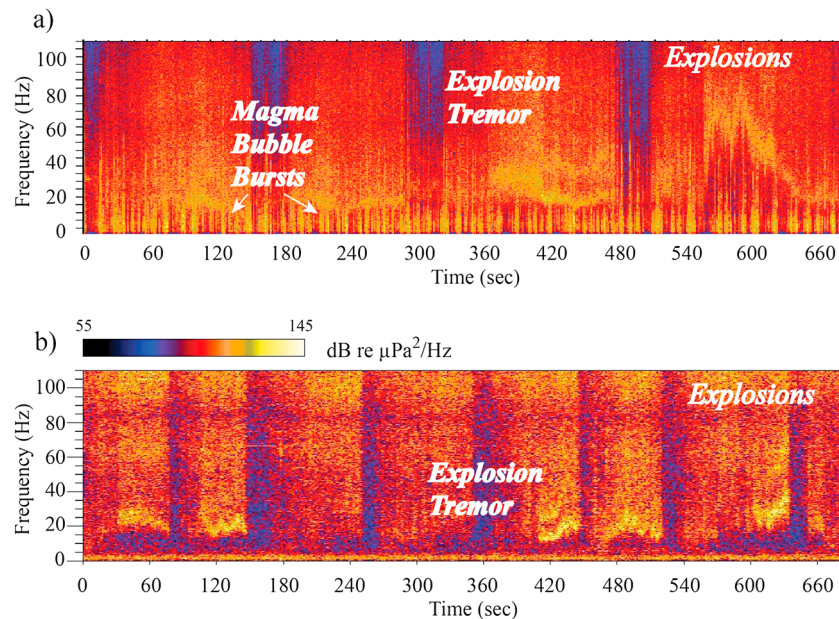
Figure 2. Spectrograms from (a) an in situ hydrophone (a GreenRidge Sciences Bprobe™) deployed at the summit of West Mata Volcano near *Hades* vent and (b) moored hydrophone ~4 km south of the volcano. In situ hydrophone shows low-frequency (1–40 Hz), short-duration signals likely caused by magma bubble bursts from *Hades* vent. Both hydrophones exhibit examples of diffuse, broadband explosions, and tremor. Diffuse explosions and tremor are likely caused by violent degassing at the *Prometheus* vent. Color bar shows decibel level for both spectrograms.

Harmonic tremor is occasionally observed within these degassing episodes, with fundamental frequencies between 20 and 100 Hz (Figures 2a and 2b). Volcanic tremor may be caused by a wide range of processes, including resonance [e.g., *Chouet*, 1988; *Lees et al.*, 2004], unsteady fluid flow [*Julian*, 1994], and repeated stick-slip events [*Dmitrieva et al.*, 2013; *Hotovec et al.*, 2013]. Tremor at West Mata occurs in concert with the degassing events; the broadband degassing signal and the narrowband tremor often begin and end at the same time, although the frequency of the tremor may vary within a given pulse. This strongly suggests that the tremor is associated with gas release during the episodic gas-release events.

During the ROV dives in May 2009, the in situ hydrophone was deployed ~25 m from the *Hades* vent and ~100 m from *Prometheus* vent. In addition to detecting the fragmentation degassing episodes associated with *Prometheus*, the hydrophone recorded a series of lower frequency (1-40 Hz), impulsive acoustic arrivals consistent with magma bubble burst explosions originating at *Hades* (Figure 2a). Coincident video shows that the Hades vent exhibited extended (minutes to hours) periods of magma gas bubble generation, typically 50–100 cm in radius, producing dozens to hundreds of bubble bursts per hour. The proximity of the in situ hydrophone to *Hades* allows the recordings to be relatively free of multipath effects and ROV noise, and enables the direct acoustic arrival pulse to be clearly recorded. The timing on the Bprobe™ is not accurate enough to definitively correlate portions of bubble oscillations with segments of the waveform. However, it is likely that the strongest pressure signal recorded on the Bprobe™ corresponds to the largest acceleration of the bubble wall, and the downward, negative amplitude reflects the bubble collapse (Figure 3) [*Vergniolle and Brandeis*, 1996]. Subsequent signal oscillations in the hydrophone record of the bursts are likely due to signal reflections or continued oscillations due to the elastic response of the water to the original bubble burst. Although the timing is not definitive, this good correlation between the acoustic and video records of a deep ocean degassing eruption is highly unusual and was not as clear on similar records from NW Rota-1 in the Mariana Arc [*Chadwick et al.*, 2008].

4. Eruption Dynamics and Evolution

Regional hydrophone recordings from the southern Lau Basin (~20.5°S, 176.75°W) indicated that the West Mata eruption continued between the time of the initial ROV visit in May 2009 and the deployment of the local hydrophone array in December 2009, increasing temporarily in intensity in the wake of the M_w 8.1 Great
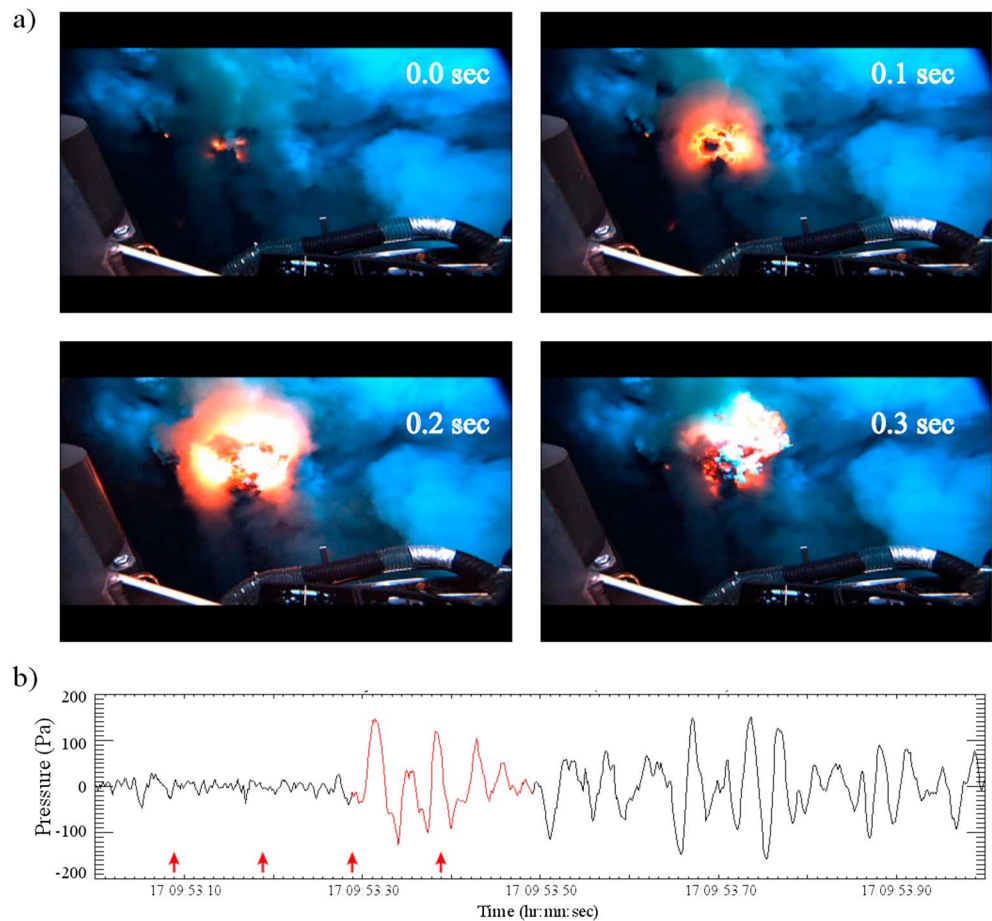
Figure 3. (a) Video image sequence of a magma gas bubble burst at West Mata Volcano summit vent *Hades* taken by the *Jason-2* ROV [*Resing et al.*, 2011; *Rubin et al.*, 2012]. First three frames show growth of the bubble; final frame is collapse. Time shown is relative to first frame. (b) Acoustic time series of bubble growth and burst recorded by Bprobe™ hydrophone deployed 25 m from vent. Red arrows show time of the four still images in Figure 3a. No pressure signal is detected as bubble grows (frames 1–3), bubble burst causes first pressure signal peak, followed by bubble collapse (frame 4). Red part of time series shows initial bubble burst signal followed by multipath acoustic arrivals and oscillations due to response of instrument.

Samoan earthquake on 29 September 2009 [*Bohnenstiehl et al.*, 2014]. Between December 2009 and early July 2010, broadband degassing signals observed on the local hydrophone array continued with similar rates and durations and exhibited similar acoustic energy levels. The West Mata eruption intensity significantly declined by December 2010, becoming intermittent (2–3 explosions per day) by January 2011, and broadband degassing signals were no longer detected after February 2011. Root-mean-square (RMS) amplitude values (Figure 4, bottom) show this reduction in eruption acoustic energy levels from 2010 to 2011. To reduce the energy contributed from regional seismic activity, the RMS amplitudes were also high-pass filtered at 10 Hz. Despite the apparent end to explosive degassing eruptions, it is possible that effusive eruption activity may have continued after February 2011, producing sounds below the detection threshold of the moored hydrophones. However, the relatively elevated RMS levels seen in June–July 2011 (Figure 4, bottom) are very likely due to a significant increase in whale vocalizations in the region during this time, where there are day-long periods with nearly continual vocalizations from minke and fin whales in the 20–40 Hz band. Water column sensors, analysis of gas samples in the overlying hydrothermal plume, and ROV observations all confirm a complete hiatus of activity by September 2012 [*Embley et al.*, 2014].

The long-term spectrogram (Figure 4, top) also appears to show high-frequency (>30 Hz) tremor-like bands of energy; however, this tremor is not directly related to a volcanic process. These bands are a result of interference caused by multipath sea surface and seafloor reflected acoustic phases that arrive at the
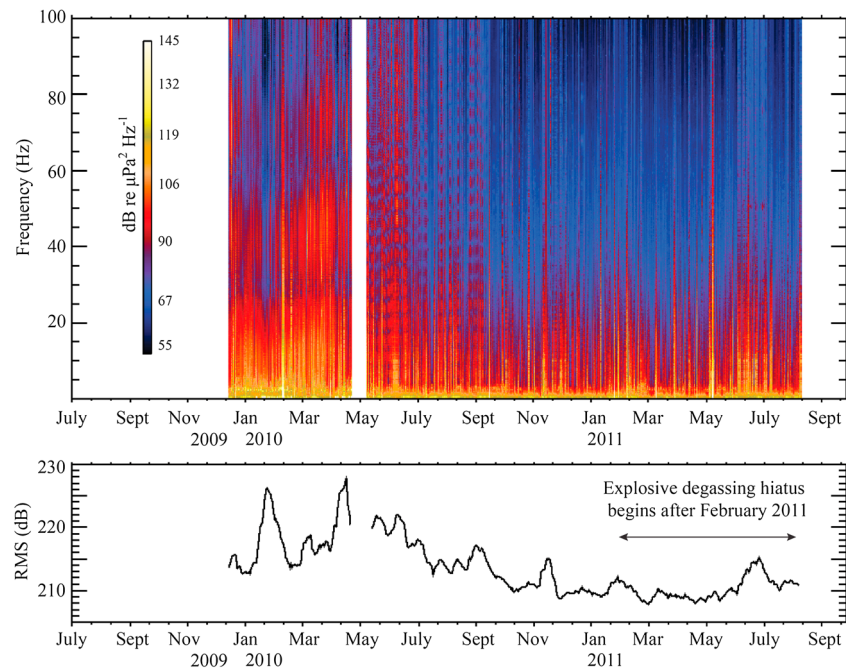
Figure 4. (top) A spectrogram of West Mata hydrophone data from December 2009 to August 2011 recorded by the southern hydrophone. The record is dominated by volcanic explosions (yellow-red repetitive broadband signals). (bottom) Daily-averaged RMS hydrophone amplitude; <10 Hz energy was filtered to remove regional seismic energy. West Mata explosions are repetitive, broadband signals. Harmonic banding is an interference pattern caused by multipathing of acoustic phases; difference in harmonic spacing is due to different hydrophone deployment depths. The West Mata explosive degassing eruptions significantly declined by December 2010, becoming intermittent (2–3 explosions per day) by January 2011 and cannot be detected after February 2011. RMS increased in June–July 2011 due to whale vocalization energy.

hydrophone with small time delays [e.g., *Matsumoto et al.*, 2011]. The interference patterns differ in frequency spacing between the 2009–2010 and 2010–2011 records because the hydrophones were deployed at different depths. The 2009–2010 hydrophone was moored 230 m deep, while the 2010–2011 hydrophone was 977 m deep, resulting in the observed interference band spacing of 32 Hz and 4.2 Hz, respectively (Figure 4).

5. Ash and Acoustic Eruption Records

Observations at other actively erupting volcanoes found episodically occurring turbidity plumes tens to hundreds of meters thick on volcano flanks (e.g., NW Rota-1 [*Walker et al.*, 2008], Monowai [*Wright et al.*, 2008], and Kavachi [*Baker et al.*, 2002]). At each of these volcanoes, flank plumes were observed at multiple locations around the edifice and from summit to seafloor, regardless of where on the summit the eruptive vent was located. These plumes did not contain hydrothermal tracers and were hypothesized to result from gravitational debris flows triggered by either eruption events or by occasional slope failures of accumulated volcanic deposits near a volcano summit. To further investigate this hypothesis, a turbidity/temperature sensor (Miniature Autonomous Plume Recorder or MAPR) was added to the southern hydrophone mooring at a depth of 2230 m (550 m above the seafloor). The MAPR sampled at 5 min intervals from December 2009 to April 2010.

In the 2009–2010 hydrophone record, the summit explosion intensity builds until an abrupt drop at the beginning of April 2010 (Figure 5a). Note that we only consider the signals >20 Hz in the spectrogram as representing energy from summit explosions since lower frequencies can be dominated by earthquake swarms and/or whale calls. We compared this time series with the water column turbidity recorded from the MAPR (Figure 5b). Unlike the acoustic record, the turbidity record is punctuated by episodes of distinct events culminating in a several day interval near the end of the record with backscatter intensities that exceeded the sensor maximum (Nephelometric Turbidity Units = 5). The turbidity maxima during each episode commonly varied with semidiurnal temperature fluctuations, possibly because internal waves moved turbidity layers up
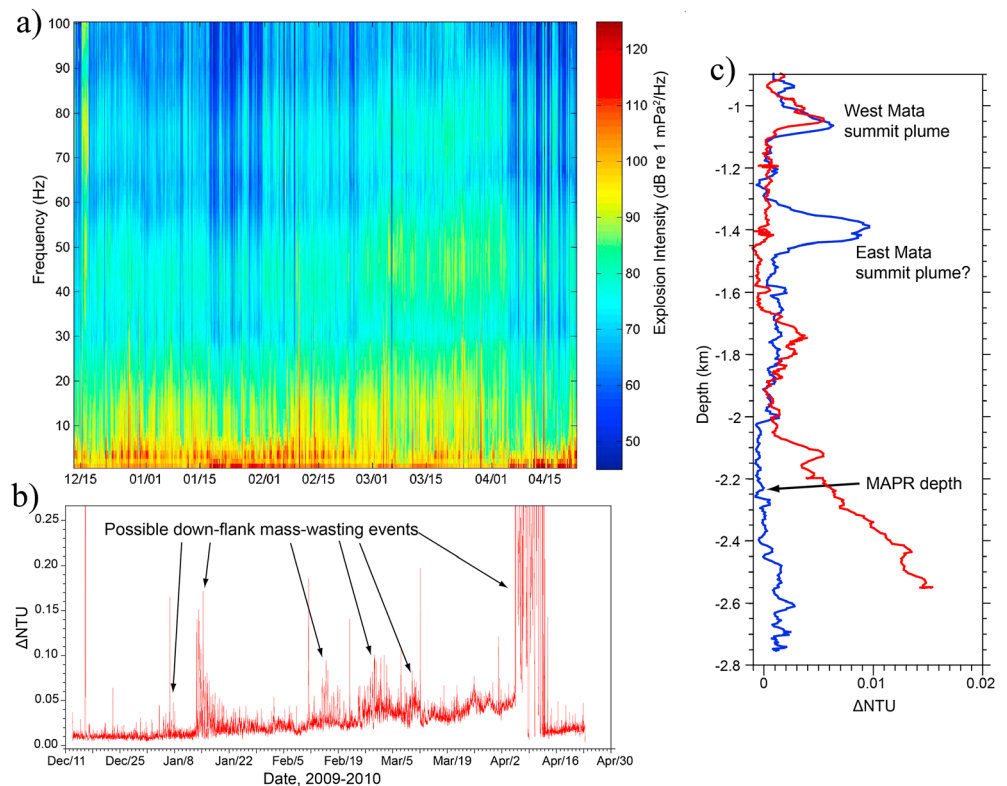
Figure 5. Comparison of (a) 5 month acoustic record to (b) MAPR turbidity record at 2230 m depth on south mooring from December 2009 to May 2010. The explosion intensity shows a clear increase between 1 March and 1 April (brighter yellow) over a broad frequency range. The turbidity record shows a gradual increase (likely from slow fouling of the detector), punctuated by at least six instances of turbidity spikes, interpreted to be down-flank mass-wasting events. (c) Turbidity profiles south of West Mata, 5 km northeast of the mooring location, 5 May 2010 (red line), and at the mooring location, September 2012 (blue line). Note that the baseline ΔNTU value at the beginning and end of the MAPR record was ~0.01, similar to the 2010 profile ΔNTU at the same depth. By 2012, the deep turbidity layer (<~2000 m) seen in 2010 (and 2008) around West Mata was absent at the mooring location as well as on profiles 12 km southeast and southwest of West Mata, implying a hiatus in the supply of fine particles from the flanks of West Mata.

and down as they dispersed. Laboratory calibrations using polystyrene and natural clay particles suspended in fresh water show that particle mass concentrations, C, are a linear function of NTU [*Baker et al.*, 2001]. For particles with an equivalent spherical diameter of 0.1–5 μm, $C = a*NTU$, where a ranges from 0.3 to 1.2 mg/L. C values in the West Mata plumes could thus range from ~0.1 mg/L in the weaker events to ~4 mg/L in the early April 2010 event.

Radiometric dating of a lava sample collected from a flow near *Prometheus* vent in September 2012 indicates it was erupted in December 2010 [*Embley et al.*, 2014]. This observation combined with the moored hydrophone records led *Embley et al.* [2014] to infer that the end of explosive volcanism at West Mata likely occurred in early 2011. ROV video of the sample site shows the pillow lavas there were truncated, likely sheared during a landslide. This observation, as well as negative depth changes near the summit derived from differential bathymetric mapping between December 2010 and November 2011 led *Embley et al.* [2014] to propose that the end of summit volcanism in early 2011was accompanied, or followed by, the formation of a small summit crater and a landslide on the eastern flank. We reviewed the West Mata hydrophone records for landslide or debris flow signals, such as those described by *Caplan-Auerbach et al.* [2001, 2014]. While the turbidity data collected in 2009–2010 did not correlate with observed landslides, *Caplan-Auerbach et al.* [2014] show that most slides at that time originated on West Mata's north flank and that south flank landslides would not have been well recorded by the 2009–2010 hydrophone network. The single hydrophone in 2010–2011 was deployed such that slides were more easily visible in the hydroacoustic record. With only a single hydrophone, we cannot confirm which of the events had their source on the south flank, but some events were likely associated with the observed bathymetric changes noted by *Embley et al.* [2014].

Nevertheless, it is still plausible that the distinct turbidity maxima in the 2009–2010 MAPRS data result from plumes that originated as occasional south flank slope failures triggered by debris accumulations during eruption intervals. This view is consistent with the fact that the largest turbidity event occurred just days after a long period of increased explosive activity throughout March 2010. The observation that a widespread bottom turbidity layer that was seen in 2008 and 2010, was absent in 2012 (Figure 5c), implies that the West Mata eruption was an important contributor to nonbiogenic sediment deposition in the NE Lau Basin during this period.

6. Summary

In situ hydrophones deployed on West Mata in 2009 and moored hydrophones deployed between December 2009 and August 2011 all captured the submarine volcano in a mode of active magmatic degassing and expulsion of ash. The eruptive degassing formed ~50–100 cm radius lava bubbles at *Hades* vent (observed via ROV; *Resing et al.* [2011]) that produced low-frequency (1–40 Hz), short-duration bubble-burst signals. The *Prometheus* vent exhibited lava episodic fragmentation and broadband acoustic signals with volcanic tremor. Our unique 20 month long moored hydrophone record shows the evolution of activity at the volcano, ranging from explosive degassing eruptions during the first mooring deployment in December 2009, through a several month period of decline, becoming intermittent (2–3 explosions per day) by January 2011, to an absence of detectable degassing explosions by February 2011. Despite the apparent end to explosive degassing eruptions, it is possible that effusive eruption activity continued after February 2011 but produced sounds below the detection threshold of the moored hydrophones.

Synchronous hydrophone and turbidity data during the first 5 months show a near-continuous record of summit explosions punctuated by occasional increases in turbidity in the deep water column. It is our interpretation that the hydrophone and MAPR record from 2009 to 2010 shows a process of continual eruption of gas and ash, leading to small-scale debris flows that help construct the volcanic edifice and fed a widespread bottom turbidity layer. The large summit depression evident from bathymetric differencing [*Embley et al.*, 2014] may have been a single, large slide that occurred outside of the time that our turbidity sensor was recording.

West Mata Volcano and NW Rota-1, in the Mariana Arc, are the only two deep ocean volcanoes where degassing eruptions have been visually observed and simultaneously recorded by in situ hydrophones. Video comparison of *Brimstone* vent at NW Rota-1 [*Chadwick et al.*, 2008] and *Hades* shows these vents also have different degassing eruption styles. NW Rota-1 exhibits rapid and chaotic degassing without formation of prolonged, large (>50 cm) magma bubbles. At NW Rota-1, the degassing bursts were very difficult to correlate with the hydrophone records because of near simultaneous, multiple, rapid bursts. In contrast, *Hades* produced clear acoustic signals correlated to the relatively slow inflation and subsequent implosion of the gas bubbles. This eruption character may allow us in the future to use acoustic techniques [*Dziak et al.*, 2012] to estimate gas fluxes and compare these directly to video estimates of the bubble volumes from the eruption.

References

Baker, E. T., D. A. Tennant, R. A. Feely, G. T. Lebon, and S. L. Walker (2001), Field and laboratory studies on the effect of particle size and composition on optical backscattering measurements in hydrothermal plumes, *Deep Sea Res., Part I*, 48, 593–604.

Baker, E. T., G. J. Massoth, C. E. J. de Ronde, J. E. Lupton, and B. I. A. McInnes (2002), Observations and sampling of an ongoing subsurface eruption of Kavachi Volcano, Solomon Islands, May 2000, *Geology*, 30, 975–978.

Bevis, M., et al. (1995), Geodetic observations of very rapid convergence and back-arc extension at the Tonga Arc, *Nature*, 374, 249–251, doi:10.1038/374249a0.

Bohnenstiehl, D. R., R. P. Dziak, H. Matsumoto, and J. A. Conder (2014), Acoustic response of submarine volcanoes in the Tofua Arc and northern Lau Basin to two great earthquakes, *Geophys. J. Int.*, 196, 1657–1675, doi:10.1093/gji/ggt472.

Caplan-Auerbach, J., C. G. Fox, and F. Duennebier (2001), Hydroacoustic detection of submarine landslides on Kilauea Volcano, *Geophys. Res. Lett.*, 28, 1811–1813, doi:10.1029/2000GL012545.

Caplan-Auerbach, J., R. P. Dziak, D. R. Bohnenstiehl, W. W. Chadwick, and T.-K. Lau (2014), Hydroacoustic investigation of submarine landslides at West Mata Volcano, Lau Basin, *Geophys. Res. Lett.*, 41, 5927–5934, doi:10.1002/2014GL060964.

Chadwick, W. W., Jr., K. V. Cashman, R. W. Embley, H. Matsumoto, R. P. Dziak, C. E. J. de Ronde, T. K. Lau, N. D. Deardorff, and S. G. Merle (2008), Direct video and hydrophone observations of submarine explosive eruptions at NW Rota-1 Volcano, Mariana Arc, *J. Geophys. Res.*, 113, B07S10, doi:10.1029/2007JB005215.

Chouet, B. (1988), Resonance of a fluid-driven crack: Radiation properties and implications for the source of long-period events and harmonic tremor, *J. Geophys. Res.*, 93(B5), 4375–4400, doi:10.1029/JB093iB05p04375.

Clague, D. A., J. B. Paduan, D. W. Caress, H. Thomas, W. W. Chadwick Jr., and S. G. Merle (2011), Volcanic morphology of West Mata Volcano, NE Lau Basin, based on high-resolution bathymetry and depth changes, *Geochem. Geophys. Geosyst.*, 12, QOAF03, doi:10.1029/2011GC003791.

Dmitrieva, K., A. J. Hotovec-Ellis, S. Prejean, and E. M. Dunham (2013), Frictional-faulting model for harmonic tremor before Redoubt Volcano eruptions, *Nat. Geosci.*, 6(8), 652–656.

Dziak, R. P., E. T. Baker, A. M. Shaw, D. R. Bohnenstiehl, W. W. Chadwick Jr., J. H. Haxel, H. Matsumoto, and S. L. Walker (2012), Flux measurements of explosive degassing using a year-long record at an erupting submarine volcano, *Geochem. Geophys. Geosyst.*, 13, Q0AF07, doi:10.1029/2012GC004211.

Embley, R. W., et al. (2014), Eruptive modes and hiatus of volcanism at West Mata seamount, NE Lau Basin: 1996–2012, *Geochem. Geophys. Geosyst.*, 15, 4093–4115, doi:10.1002/2014GC005387.

Hotovec, A. J., S. G. Prejean, J. E. Vidale, and J. Gomberg (2013), Strongly gliding harmonic tremor during the 2009 eruption of Redoubt Volcano, *J. Volcanol. Geotherm. Res.*, 259, 89–99.

Julian, B. R. (1994), Volcanic tremor: Nonlinear excitation by fluid flow, *J. Geophys. Res.*, 99(B6), 11,859–11,877, doi:10.1029/93JB03129.

Keller, N. S., R. J. Arculus, J. Hermann, and S. Richards (2008), Submarine back-arc lava with arc signature: Fonualei Spreading Center, northeast Lau Basin, Tonga, *J. Geophys. Res.*, 113, B08S07, doi:10.1029/2007JB005451.

Lees, J. M., E. I. Gordeev, and M. Ripepe (2004), Explosions and periodic tremor at Karymsky Volcano, Kamchatka Russia, *Geophys. J. Int.*, 158(3), 1151–1167.

Matsumoto, H., D. R. Bohnenstiehl, J. H. Haxel, R. W. Embley, and R. P. Dziak (2011), Mapping the sound field of an erupting submarine volcano using an acoustic glider, *J. Acoust. Soc. Am.*, 129(3), 94–99, doi:10.1121/1.3547720.

Millen, D. W., and M. W. Hamburger (1998), Seismological evidence for tearing of the Pacific Plate at the northern termination of the Tonga subduction zone, *Geology*, 26, 659–662.

Resing, J. A., et al. (2011), Active submarine eruption of boninite in the northeastern Lau Basin, *Nat. Geosci.*, 4, 799–806, doi:10.1038/ngeo1275.

Rubin, K. H., S. A. Soule, W. W. Chadwick Jr., D. J. Fornari, D. A. Clague, R. W. Embley, E. T. Baker, M. R. Perfit, D. W. Caress, and R. P. Dziak (2012), Volcanic eruptions in the deep-sea, *Oceanography*, 25(1), 142–157, doi:10.5670/oceano.2012.12.

Rubin, K. H., et al. (2013), Timescale and petrogenesis of 2009 and older W. Mata boninite magmas, *Mineral. Mag.*, 77(5), 2094.

Vergniolle, S., and G. Brandeis (1996), Strombolian explosions: 1. A large bubble breaking at the surface of a lava column as a source of sound, *J. Geophys. Res.*, 101(B9), 20,433–20,447, doi:10.1029/96JB01178.

Walker, S. L., E. T. Baker, J. A. Resing, W. W. Chadwick Jr., G. T. Lebon, J. E. Lupton, and S. G. Merle (2008), Eruption-fed particle plumes and volcaniclastic deposits at a submarine volcano: NW Rota-1, Mariana Arc, *J. Geophys. Res.*, 113, B08S11, doi:10.1029/2007JB005441.

Wright, I. C., W. W. Chadwick Jr., C. E. J. de Ronde, D. Reymond, O. Hyvernaud, H.-H. Gennerich, P. Stoffers, K. Mackay, M. A. Dunkin, and S. C. Bannister (2008), Collapse and reconstruction of Monowai submarine volcano, Kermadec Arc, 1998-2004, *J. Geophys. Res.*, 113, B08S03, doi:10.1029/2007JB005138.

Zellmer, K. E., and B. Taylor (2001), A three-plate kinematic model for Lau Basin opening, *Geochem. Geophys. Geosyst.*, 2(5), 1020, doi:10.1029/2000GC000106.